fractal and fractional

MDPI

Article

Fractional Order Model Identification of a Person with Parkinson's Disease for Wheelchair Control

Mircea Ivanescu [1,*], Ioan Dumitrache [2], Nirvana Popescu [3] and Decebal Popescu [3]

[1] Department of Mechatronics, University of Craiova, 107 Decebal Street, 200776 Craiova, Romania
[2] Department of Automation, University Polytehnica of Bucharest, 060042 Bucharest, Romania
[3] Department of Computer Science, University Polytehnica of Bucharest, 060042 Bucharest, Romania
* Correspondence: ivanescu@robotics.ucv.ro

Abstract: The paper focuses on the design of an intelligent interface that compensates for the incapacity of a person with Parkinson's disease to drive a wheelchair. The fractional order model that defines a person with Parkinson's disease is investigated. An identification technique based on the analysis of the frequency behavior of the movement of a wheelchair driven by a with Parkinson's disease person on the test trajectory is proposed and a delay time crossover model with fractional order exponent $\beta = 1.5$ is inferred. The fractional dynamic model of the "disabled man-wheelchair" system is discussed and a control system is proposed to compensate for the inability of the wheelchair driver. The conditions that ensure the stability of the closed loop control system are inferred. An experimental technique for analyzing movement performance is developed and a quality index is proposed to evaluate these experiments. The values of this index on the tests performed on Parkinson's patients are analyzed and discussed.

Keywords: human fractional order model; control system; stability

Citation: Ivanescu, M.; Dumitrache, I.; Popescu, N.; Popescu, D. Fractional Order Model Identification of a Person with Parkinson's Disease for Wheelchair Control. *Fractal Fract.* **2023**, *7*, 23. https://doi.org/10.3390/fractalfract7010023

Academic Editors: Isabela Roxana Birs, Cristina I. Muresan and Clara Ionescu

Received: 14 November 2022
Revised: 19 December 2022
Accepted: 21 December 2022
Published: 26 December 2022

1. Introduction

The analysis of human behavior in control systems has been of paramount importance, becoming a focal research topic in recent decades. The mainstream literature includes numerous titles dedicated to this objective. Beginning with the pioneering paper of Mc Ruer and Kleinman [1,2] and continuing with the most recent contributions [3,4], these papers have tried to define mathematical models that characterize human dynamics in a control system. Representative papers in this field are [5,6], in which man-machine models involved in the control of vehicles are analyzed, as well as how the visual information is processed by the human operator and how the vehicle motion is controlled. Techniques and methods derived from the control theory regarding the controller type characteristics of a human operator are discussed in [7–9]. The cyber-mechanism associated with visual feedback control is analyzed in [10,11]. Different problems related to data storage and levels of human processing are formulated in [12–14]. The human control strategy based on memorizing of sequences of past observations is analyzed in [15,16]. Drawing on these observations, it is concluded that the dynamics of a human controller is more accurately described by fractional order models (FOM) that add memory components to the conventional differential model, integer order models (IOM). The Mc Ruer's crossover model for fractional order systems is generalized in [17]. The adaptive behavior of a human operator to the characteristics of the driven system is studied in article [18].

All these papers indicate that to achieve a good performance of the control system, highly accurate knowledge of the transfer function of the human operator, $Y_h(s)$, is required. Several models are proposed and used in literature. We can mention the Mc Ruer model [1], $Y_h(s) = K_p \frac{(1+T_L s)}{s(1+T_I s)} e^{-\tau s}$. In [4], the model $Y_h(s) = \frac{K_p e^{-\tau s}}{s(1+T_I s)}$ is analyzed, which is developed

in [5] as $Y_h(s) = \frac{K_p e^{-\tau s}}{s^{\beta}(1+T_I s)}$ with the fractional exponent $\beta = 1.2$. Other papers [7–9] examine the models $Y_h(s) = K_p \frac{(1+T_L s)e^{-\tau s}}{s(1+T_I s)(1+T_N s)}$ or $Y_h(s) = \frac{k_p e^{-\tau s}}{s^{\alpha}}$ for $\propto = 0.4$.

In these models, the first component is associated with the properties of the human neuromuscular system and the second one provides the control function, defined by the operator's ability to select the optimal control parameters. People with health problems are characterized by transfer functions in which the second component is negligible or does not exist and the first component is determined by the health conditions of the people. There are a few papers in the literature that analyze the behavior of people with health problems, locomotor disabilities or brain disorders. In this context, the human neuromuscular dynamics of a disabled operator is discussed in [19]. The quality of movement in disabled man control systems is presented in [20]. Other papers [21–23] emphasize the complexity of disabled human control systems determined either by the physical or mental incapacity of the human operator.

All these papers study the human model and investigate solutions, using various techniques and procedures, to determine a control system that allows the desired performance. Thus, the fractional order models or integer order models of healthy people (HP) or disabled people (DP) are analyzed and various design techniques are proposed, ranging from the classic design methods for closed loop control to associated methods of cyber-physical systems. These are completed by the implementation of controllers, either by integer order models (IOMC) or by fractional order models (FOMC). A selection of these papers is presented in Table 1.

Table 1. Man-machine systems: models, control techniques.

Paper	Healthy/Disability Man	Man Model	Control Techniques	Controller
[1,2,8,18]	HP	Linear IOM	Classic Closed Loop Control	IOMC
[3,11]	HP	Linear IOM	Fuzzy Control	IOMC
[12,16,23]	HP	Linear FOM with time delays	Optimal control techniques	IOMC
[4,6]	HP	Linear FOM with time delays	Classic Closed Loop Control	FOMC
[13,14,17,21]	HP	Nonlinear FOM with time delays	Cyber-physical control	IOMC
[7,23,24]	HP	FOM	Admitance control	IOMC
[19]	HP	FOM	Frequency techniques	IOMC
[5,20]	HP	Nonlinear IOM with time delays	Algebraic criteria	IOMC
[9,10,25]	HP	Linear IOM with time delays	Classic Closed Loop Control	IOMC
Our paper	DP	Linear FOM with time delays	Lyapunov techniques and frequency criteria	FOMC or IOMC

In general, human behavior is assimilated through a two-component transfer function (Figure 1). The first component is known as the crossover model [1,4] and is defined by the transfer function

$$Y_h(s) = \frac{x_h(s)}{x_{target}(s)} = \frac{k_h}{s} \tag{1}$$

where x_{target} defines the target variable and x_h is the human action. The second component corresponds to the adaptive characteristic of the human operator, a self-tunning component, $Y_{ST}(s)$, through which the operator compensates the characteristics of the driven system [24].

$$Y_{ST}(s) = \frac{1}{Y_v(s)} \tag{2}$$

where $Y_v(s)$ represents the wheelchair transfer function. The open-loop transfer function will be:

$$Y(s) = Y_h(s)\,\frac{1}{Y_v(s)}Y_v(s) = \frac{k_h}{s} \tag{3}$$

which ensures the desired performances in the closed-loop control system.

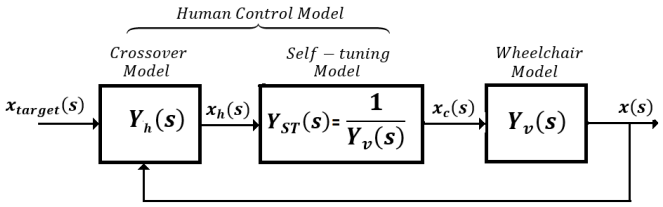

Figure 1. Closed-loop control with human operator.

In case of people with disabilities, the control system changes (Figure 2). The first component $Y_h(s)$ becomes a fractional exponent transfer function:

$$Y_h(s) = \frac{k_h}{s^\beta} \tag{4}$$

where k_h and β are the parameters that characterize the degree of physical and mental deficiency of the human operator (persons with arm or leg-emphasized hemiparesis, with severe brain damage). In most cases, this incapacity eliminates the self-tuning component of the operator, $Y_{ST}(s)$, (Figure 2b), completely. The open-loop transfer function becomes:

$$Y(s) = \frac{k_h}{s^\beta}Y_v(s) \tag{5}$$

and the quality of motion worsens. A controller must be inserted into the closed-loop control system to obtain the desired quality of wheelchair movement [24,25].

Our paper falls within this area of investigation, analyzing and proposing an intelligent control system that compensates for this incapacity of a disabled man with Parkinson's disease who drives a wheelchair. This health condition of the driver with Parkinson's disease can lead to a reduced stability of the wheelchair movement. Our research focuses on identifying a fractional model for the people with Parkinson's disease, assuming that such models define more accurately the dynamic characteristics of people with this class of disability. Based on this model, a control algorithm has been proposed in our paper to satisfy the desired performances. The main results can be summarized as follows:

- The fractional order model that defines a Parkinson's is investigated. An identification technique based on the analysis of the frequency behavior of the movement of a wheelchair driven by a person with Parkinson's disease on the test trajectory is proposed. A fractional order exponent $\beta = 1.5$ is inferred for people with this class of disability and a delay time crossover model is proposed.
- The fractional dynamic model of the "disabled person-wheelchair" system is discussed.
- An intelligent control system is proposed to compensate for the inability of the wheelchair driver. The stability of the control system is demonstrated by the Lyapunov techniques and frequency criteria derived from Yakubovici-Kalman-Popov Lemma.
- An experimental technique for analyzing the movement performance is developed and a quality index is proposed to evaluate these experiments. The values of this index on the tests performed on Parkinson's patients are analyzed and discussed.

The paper is structured as follows: Section 2 presents Materials and Methods with subsections on Disabled Human Model Identification Technique, Disabled Person-Wheelchair Fractional Order Model and Control Systems, Section 3 emphasizes the Results with sub-

sections on Numerical Simulations and Experimental Tests, and Section 4 is devoted to Discussions and Conclusions.

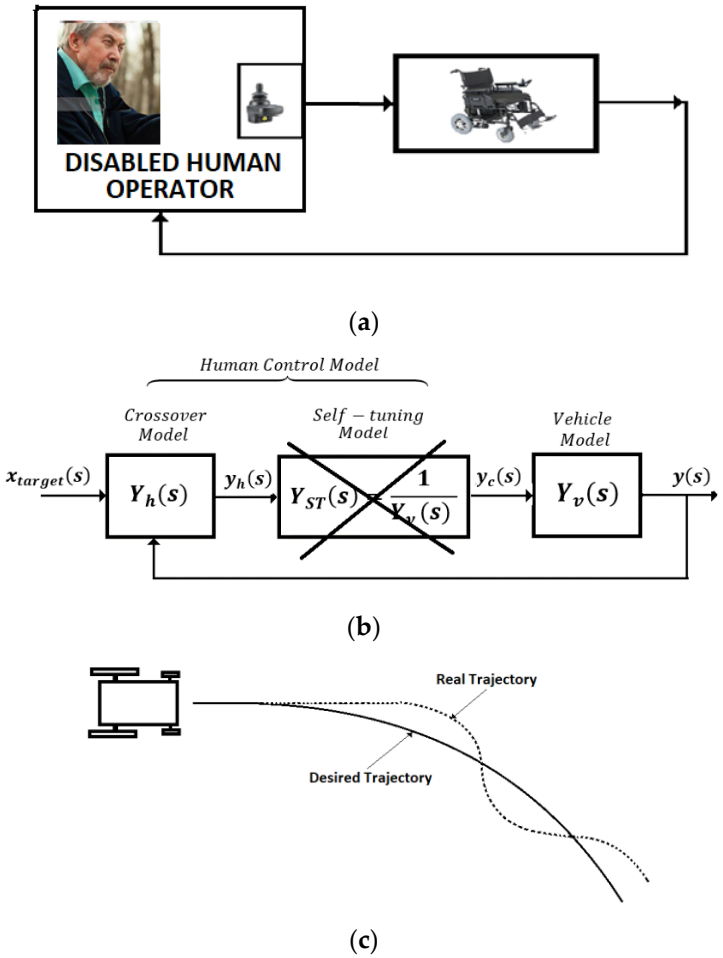

Figure 2. (**a**) Closed-Loop Control with human operator with disabilities. (**b**) Transfer functions for the Closed-Loop Control with disabled human operator. (**c**) Dynamic behavior of the disabled operator's wheelchair.

2. Materials and Methods

2.1. Disabled Human Operator Identification

The identification of a human operator model was performed on a patient, a human operator with Parkinson's disease, driving a wheelchair on an imposed path. The wheelchair is an EZ Lite Cruiser Standard Model [26] with rear wheel drive and a brushless motor to power them. A joystick and a conventional control system are used to ensure the direction of control and the velocity. The identification technique uses a data acquisition and processing system implemented by a Raspberry Pi4 system (Figure 3). An experiment was used in which the operator, a man with no mental disabilities, whose driving performance was severely impaired by the lack of controllability of hand movement caused by Parkinson's disease, was asked to drive the wheelchair on an imposed trajectory with a certain degree of difficulty. It was considered representative for the evolution on a trajectory that suddenly changes the direction of motion at right angles, as seen in Figure 4. The output characteristic of the "person with Parkinson' disease-wheelchair" system is analyzed for an evolution on a test trajectory. A test trajectory is considered a motion at which, at a given moment, the direction of movement is switched with 90° (step input, $x_{target} = \frac{\pi}{2}$). The output of the system is considered the rotation θ around its instantaneous centre of rotation (ICR) [25,26].

This variable is determined from the angular velocities ω_L, ω_R measured by the wheelchair velocity sensors and stored in the Data Acquisition Module.

$$\theta = k_\theta(\omega_L - \omega_R) \tag{6}$$

An experiment consists of the sequences of movement through which the wheelchair, driven by a man with Parkinson's disease (the operator), moves on a test trajectory. The motion on a test trajectory requires a sudden 90° change of direction, a change made by accelerating one wheel and decelerating the opposite wheel. When reaching the new direction, the operator returns the velocities to the same value maintaining the motion on the new direction. Throughout the experiment, the angular velocities are measured and stored. Subsequently, these parameters are transferred to a computer and analyzed. MATLAB toolboxes (R2020a) are used to determine the family of output characteristics $\{\theta(t), t\}_i$ and frequency characteristics (Bode diagram). The experiments were conducted on two patients without mental disabilities who had the intellectual ability and the capacity to drive a wheelchair to a target, but whose driving performance was severely impaired by the lack of controllability of hand movement caused by Parkinson's disease. A number of 20 tests are performed independently by two patients with Parkinson's disease to obtain an accurate estimate of the parameters of the "disabled person-wheelchair" model. Figures 5–7 provide the representation of the output variable θ(t) for the 10 experiments (Figure 5—Patient 1) and the Bode diagram (Figures 6 and 7). The results of the experiments are summarized in Table A1 (Appendix A).

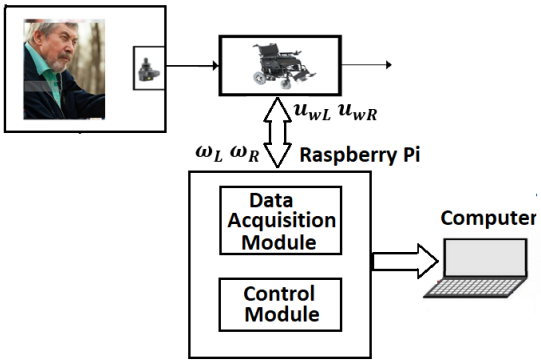

Figure 3. Data acquisition and control system.

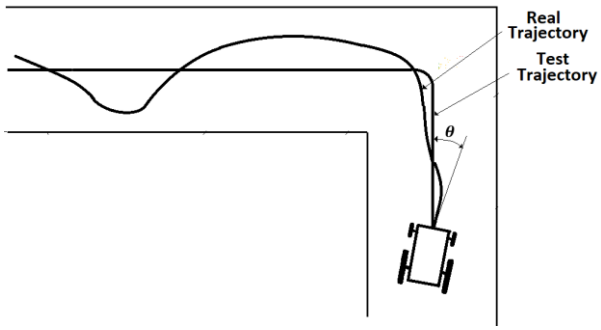

Figure 4. Test space for model identification.

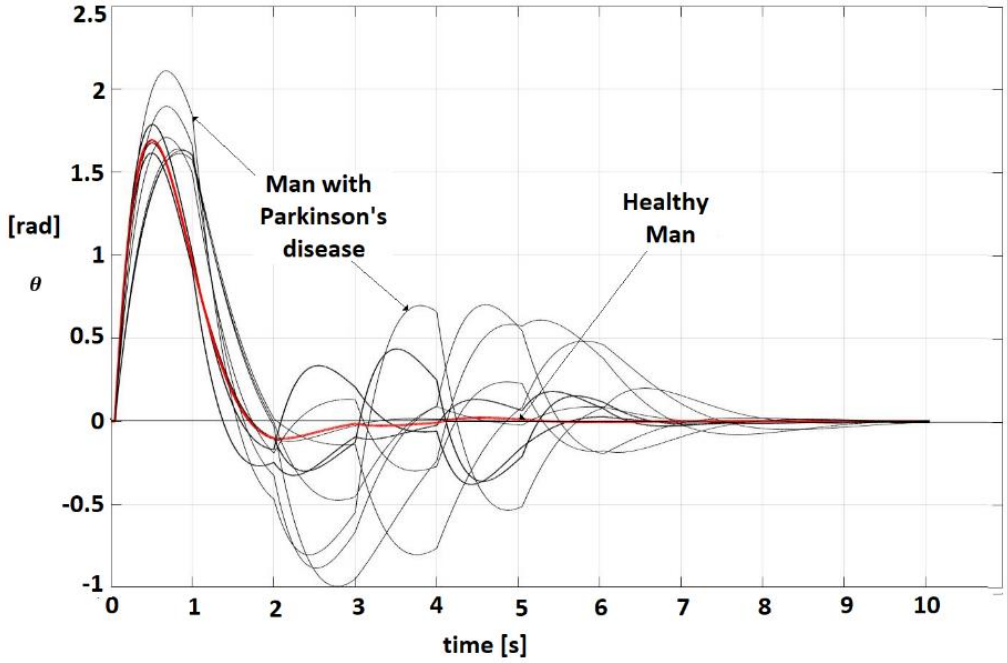

Figure 5. Output characteristics $\{\theta(t),\, t\}_i$ (Man with Parkinson's disease—black line, Healthy Man—red line).

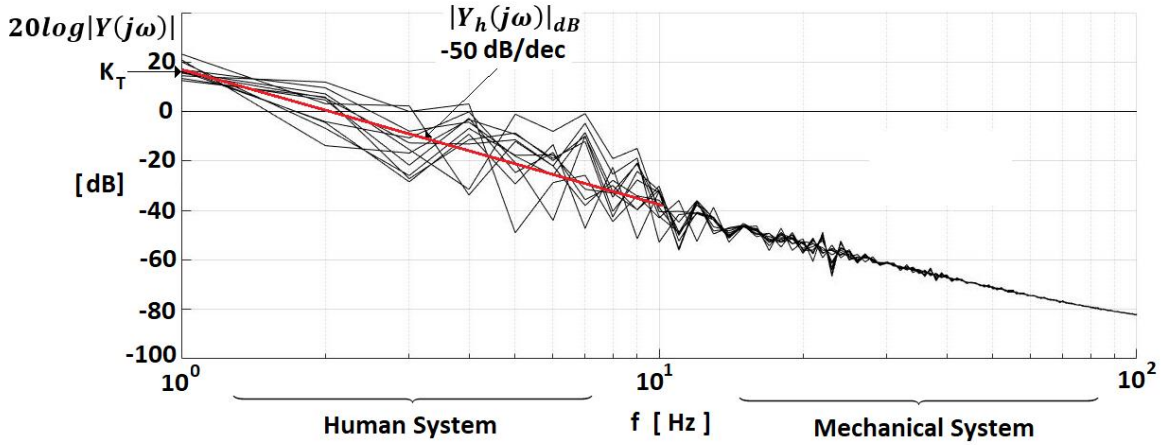

Figure 6. Bode diagram: Magnitude—frequency plot (Man with Parkinson's disease).

The analysis of the curve family $\{\theta(t),\, t\}_i$ does not only indicate the somewhat chaotic evolution of the global system, whose characteristics is determined by the incapacity of the disabled operator, but it also shows the tendency for a good evolution towards the target position. The Bode diagrams, Magnitude-frequency (Figure 6) and Phase-frequency (Figure 7), show the behavior of the "person-wheelchair" system with transfer function:

$$Y(s) = \frac{\theta(s)}{x_{targ}(s)} = Y_h(s)\; Y_v(s) \tag{7}$$

For low frequency ($f \in [1,\, 10]$ Hz), the electro-mechanical component can be neglected, $Y(s) \approx Y_h(s)$. The human behavior for a step input, $x_{target}(s) = \frac{\pi}{2s}$, is evaluated by the magnitude-frequency plot for $f \in [1,\, 10]$ Hz with a slope that can be estimated at

-50 dB/dec and the phase-frequency plot at a value of $\varphi \cong -3.925\ [rad] \cong -2.5\frac{\pi}{2}\ [rad]$ (Table A1).

$$\theta(s) = \frac{k_h}{s^\beta}\frac{\pi}{2s} = \frac{k_T}{s^{2.5}} \tag{8}$$

which determines the identification of the human behavior by the transfer function $Y_h(s) = \frac{k_h}{s^\beta}$ with the fractional exponent $\beta = 1.5$ and the human gain coefficient $k_h = 9.54$ as the average value shown in Table A1.

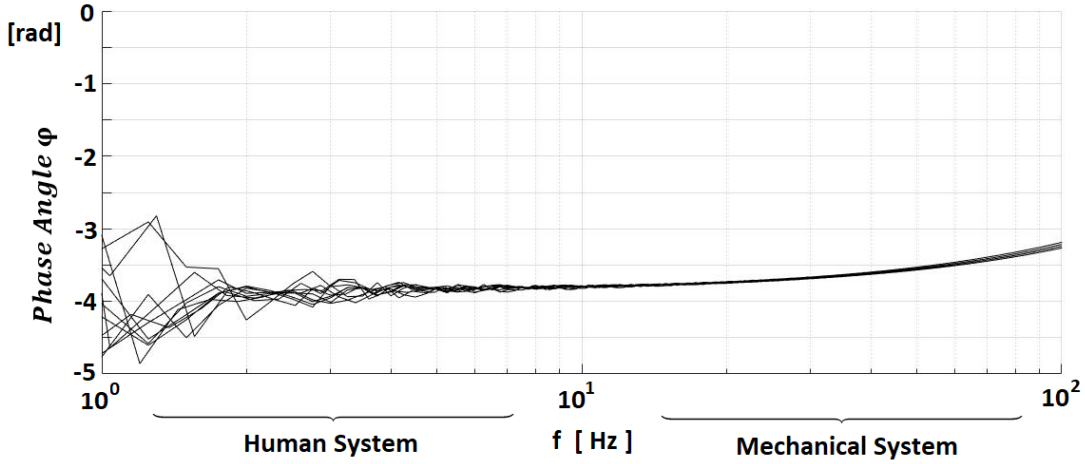

Figure 7. Bode diagram: Phase—frequency plot, (Man with Parkinson's disease).

Remark 1. *The response time of the disabled operator determined by the propagation time in the nervous system, as well as the time constants of the muscular system, introduces a delay component* τ *[6,11]. Through this component, the dynamic model becomes:*

$$Y_h(s) = \frac{k_h}{s^\beta}e^{-\tau s} \tag{9}$$

Assumption 1 *The following inequality will be considered for the delay time components*

$$z^T(t)z(t-\tau) \le \rho_M z^T(t)z(t) \tag{10}$$

where ρ_M *is a positive constant.*

It is very difficult to evaluate this time delay. Experimental results [11] allow us to use $\tau = 0.1$ s and identify a domain $\Im = [0.05; 0.15]s$, $\tau \in \Im$.

Remark 2. *It is difficult to make a comparison of the model (9) with similar models in the literature as all papers refer to healthy operators with no physical or mental disabilities. We can mention:* $Y_h(s) = \frac{\omega_c}{s}e^{-\tau s}$, *or* $Y_h(s) = K_p\frac{(1+T_L s)}{s(1+T_I s)}e^{-\tau s}$ *from [1], the models* $Y_h(s) = \frac{K_p e^{-\tau s}}{s(1+T_I s)}$, $Y_h(s) = \frac{K_p e^{-\tau s}}{s^\beta(1+T_I s)}$ *from [4,5] with the fractional exponent* $\beta = 0.8$. *Other papers [7–9] studied the models* $Y_h(s) = K_p\frac{(1+T_L s)e^{-\tau s}}{s(1+T_I s)(1+T_N s)}$ *or* $Y_h(s) = \frac{k_p e^{-\tau s}}{s^\alpha}$ *for* $\propto = 0.4$. *An analysis of the models in [4,5,7–9] indicates the use of fractional order operators to describe the dynamic behavior of healthy drivers, physically and mentally capable to perform the functions required to drive a vehicle. Our paper examines patients who had the intellectual ability and capacity to drive a wheelchair to a target, but whose driving performance was severely impaired by the lack of controllability of hand movement caused by Parkinson's disease. Comparing these models with (9), we notice the presence of the component* $\frac{1}{s^\beta}$, *the major difference being given by the fractional exponent that reaches, in the case of our model for the human operator with disabilities, the highest value* $\beta = 1.5$.

2.2. Disabled Man-Wheelchair Fractional Order Model

From (9), the human dynamics can be rewritten as:

$$Y_h(s) = \frac{x_h(s)}{x_{target}(s)} = \frac{k_h}{s^{\beta}} e^{-\tau s},\ y_h(s) = x_h(s) \tag{11}$$

where $y_h(s)$ and $x_h(s)$ are the output and the state of the human operator, respectively. Rewritting (11) in time, it yields:

$$D^{\beta} x_h(t) = k_h x_{targ}(t-\tau) \tag{12}$$

where $D^{\beta} x_h(t)$ is the Caputo fractional order derivative. In the human model, the delay variables are represented by the input $x_{targ}(t-\tau)$ and the velocity feedback $\omega_1(t-\tau)$, $\omega_2(t-\tau)$ determined by the human reaction capacity.

The dynamic model of the Disabled Person Wheelchair (DPW) is a conventional wheelchair model [26,27] with the control of velocity and motion direction given by the joystick, with a decoupled drive system and with symmetrical, electrical and mechanical, architecture, for moving to the left and, respectively, to the right. This symmetry allows to decouple the DPW model as:

$$\dot{v}^j(t) = A_v v^j(t) + b_v u_v^j(t),\ \ j = 1,2 \tag{13}$$

$$A_v = \begin{bmatrix} -R/L & -k_e/L \\ k_t/nJ & -\nu/J \end{bmatrix},\ b_v = \begin{bmatrix} 1/L \\ 0 \end{bmatrix},\ j = 1,2 \tag{14}$$

where $v^j = \begin{bmatrix} i_j\ \omega_j \end{bmatrix}^T$ defines the wheelchair state, u_v^j is the input variable (index $j = 1,\ 2$ identifies the motion direction, toward the left and right) and $R, L,\ J,\ k_t,\ k_e,\ n,\ \nu$ are the electrical and mechanical parameters of the system (Table A2). A fractional order state vector z^j is introduced and the following relations are inferred:

$$\begin{array}{l} z_1 = x_h;\ D^{0.5} z_1 = z_2;\ D^{0.5} z_2 = z_3; D^{0.5} z_3 = k_h x_{targ}(t-\tau) - k_v(\omega_1(t-\tau) - \omega_2(t-\tau)); \\ z_4^j = i_j;\ D^{0.5} z_4^j = z_5^j; D^{0.5} z_5^j = -R/L z_4^j - k_e/L\ \ z_6^j + 1/L\ u_c^j \\ z_6^j = \omega_j;\ D^{0.5} z_6^j = z_7^j; D^{0.5} z_7^j = k_t/nJ z_4^j - \nu/J\ z_6^j,\ D^{0.5} z_7^j = \dot{\omega}_j,\ j = 1,2 \\ z = \begin{bmatrix} z_1\ z_2\ z_3\ \ z_4^1\ z_5^1\ z_6^1\ z_7^1\ z_4^2\ z_5^2\ z_6^2\ z_7^2 \end{bmatrix}^T \end{array} \tag{15}$$

The fractional order model will be [28–31]

$$D^{0.5} z(t) = A_0 z(t) + A_1 z(t-\tau) + b u_c(t) + d\ x_{targ}(t-\tau) \tag{16}$$

with initial conditions

$$z(t) = \varphi(t),\ t \in [-\tau, 0] \tag{17}$$

Consider the following output variable

$$y(t) = c^T z(t) \tag{18}$$

where

$$A_0 = \begin{bmatrix} 0_{2\times1} & I_{2\times2} & & 0_{3\times4} & & & & 0_{3\times4} \\ & & 0 & 1 & 0 & 0 & & \\ & 0_{5\times3} & -R/L & 0 & \frac{-k_e}{L} & 0 & & 0_{4\times4} \\ & & 0 & 0 & 0 & 1 & & \\ & & k_t/nJ & 0 & \frac{-\nu}{J} & 0 & & \\ & & & & & & 0 & 1 & 0 & 0 \\ 0_{4\times3} & & & 0_{4\times4} & & & -R/L & 0 & \frac{-k_e}{L} & 0 \\ & & & & & & 0 & 0 & 0 & 1 \\ & & & & & & k_t/nJ & 0 & \frac{-\nu}{J} & 0 \end{bmatrix} \tag{19}$$

$$A_1 = \begin{bmatrix} & & 0_{2\times 11} & & & \\ 0_{1\times 5} & -c_v^1 & 0_{1\times 3} & -c_v^2 & 0 & \\ & & 0_{8\times 11} & & & \end{bmatrix}; b = \begin{bmatrix} 0_{4\times 1} \\ \frac{1}{L} \\ 0_{3\times 1} \\ \frac{1}{L} \\ 0_{2\times 1} \end{bmatrix}; \tag{20}$$

$$d = \begin{bmatrix} 0_{2\times 1} \\ k_h \\ 0_{8\times 1} \end{bmatrix} \tag{21}$$

$$c = [-k_{h1} \;\; k_{h2} \;\; 0_{1\times 2} \;\; -k_{\omega 1} \;\; -k_{\omega 2} \;\; 0_{1\times 2} \;\; -k_{\omega 1} \;\; -k_{\omega 2} \; 0]^T \tag{22}$$

2.3. Control System

In the wheelchair control system, the human operator based on visual information controls the direction and velocity of motion through the joystick, adapting the control to the external disturbances and maintaining the motion on an imposed trajectory. In the case of a disabled operator control, the adaptive control component and decision-making capacity are missing or largely attenuated. Consequently, the movement has a chaotic, oscillating character (Figure 4).

The proposed control system is shown in Figure 8. This system includes, in addition to the local control systems of the two active wheels, $Y_v^1(s)$, $Y_v^2(s)$, a controller $Y_c(s)$ that will implement the control law:

$$u_c(t) = -k_c y(t) \tag{23}$$

where

$$u_c(t) = u_{c1}(t) + u_{c2}(t) = -k_{c1} y(t) - k_{c2} y(t) \tag{24}$$

and the controller gain $k_c = k_{c1} + k_{c2}$, which is a positive constant that verifies the conditions:

$$Arg(eig\left(\left(A_0 + A_1 - k_{c1} b c^T\right)\right) > \frac{\pi}{2} \tag{25}$$

$$k_{c2}\sigma \leq 1 \tag{26}$$

and σ is a positive constant.

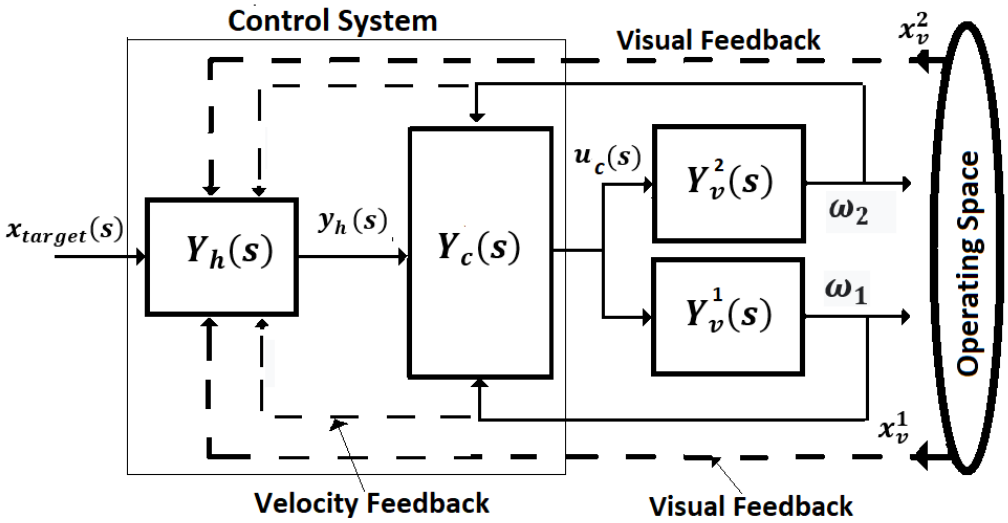

Figure 8. The control system.

Theorem 1. *The time delay fractional order system (16)–(22) with the control law (23)–(26) is asymptotically stable if the following conditions are satisfied:*

$$Arg(eig(A^*)) > \frac{\pi}{2} \tag{27}$$

$$Re\left(c^T(j\omega I - A^*)^{-1}b\right) \geq -\sqrt{\sigma} \tag{28}$$

$$\alpha = \varrho - \rho_M \rho_{A_1 P} > 0 \tag{29}$$

where $\varrho = \| \left(q + k_{c2}\sqrt{\sigma}c\right)\left(q + k_{c2}\sqrt{\sigma}c\right)^T \|$, $A^* = (A_0 + A_1 - k_{c1}bc^T)$ *is a Hurwitz matrix and* P, q *are solutions of Lyapunov equation* $\left(A^{*T}P + PA^*\right) = -qq^T$.

Proof. Assume $x_{targ}(t) = 0$, *Consider the following Lyapunov function*

$$V(z) = z^T(t)Pz(t) \tag{30}$$

where $P > 0$, $P = P^T$. The following inequalities are satisfied [32–34]

$$\lambda_{\min(P)}\|z(t)\|^2 \leq V(z) \leq \lambda_{\max(P)}\|z(t)\|^2 \tag{31}$$

The fractional order derivative is

$$D^{0.5}V(z) \leq \left(D^{0.5}z^T\right)Pz + z^TP\left(D^{0.5}z\right) \tag{32}$$

By substituting (16) into (31) yields

$$D^{0.5}V(z) \leq z^T(t)\left(A^{*T}P + PA^*\right)z(t) + z^T(t)\left(A_1^TP + PA_1\right)\Delta z(t) + 2z^T(t)Pbu_{c2}(t) \tag{33}$$

where $u_{c2} = -kc_2y$ and

$$\Delta z(t) = z(t-\tau) - z(t) \tag{34}$$

Applying the inequality (10), it is derived that

$$\|\Delta z(t)\| \leq \rho_M\|z(t)\| \tag{35}$$

By evaluating (32) along the solutions of (16)–(18), this inequality can be rewritten as

$$D^{0.5}V(z) \leq z^T\left(A^{*T}P + PA^*\right)z + 2z^T\left(Pb - \frac{1}{2}c\right)u_{c2} - \sigma {u_{c2}}^2 + \rho_M\rho_{A_1P}\|z(t)\|^2 \tag{36}$$

If the conditions (27) and (28) are verified, applying Yakubovici-Kalman-Popov Lemma [35], we have:

$$\left(A^{*T}P + PA^*\right) = -qq^T \tag{37}$$

$$Pb - \frac{1}{2}c = \sqrt{\sigma}q \tag{38}$$

Substituting (36) and (37) into (35), results into:

$$D^{0.5}V(z) \leq -z^T\left(q + k_{c2}\sqrt{\sigma}c\right)\left(q + k_{c2}\sqrt{\sigma}c\right)^Tz + \rho_M\rho_{A_1P}\|z(t)\|^2 \tag{39}$$

This inequality can be rewritten as

$$D^{0.5}V(z) \leq -\left(\varrho - \rho_M\rho_{A_1P}\right)\|z(t)\|^2$$

or by the conditions (27)–(29) results in [27,32,34]

$$D^{0.5}V(z) \leq -\alpha\|z\|^2 \tag{40}$$

□

Remark 3. *According to (23), the control law is* $PD^{0.5}$

$$u_c(t) = -k_c(c_{hc1}x_h - c_{hc2}D^{0.5}x_h - c_{c\omega 1}(\omega_1 - \omega_2) - c_{c\omega 2}D^{0.5}(\omega_1 - \omega_2)) \quad (41)$$

The terms $D^{0.5}x_h$, $D^{0.5}(\omega_1 - \omega_2)$ *represent virtual variables which can be obtained by an observer. A simpler solution is obtained by eliminating the virtual components and using only physically significant, measurable components. In this case, the component* $D^{0.5}$ ω *can be replaced by* $D^{0.5}z_7^j = \dot{\omega}_j$, *a measurable variable. Therefore, the control law becomes a classic controller PD,*

$$u_c(t) = -k_c\left(c_{hc}x_h - c_{c\omega 1}(\omega_1 - \omega_2) - c_{c\omega 2}(\dot{\omega}_1 - \dot{\omega}_2)\right) \quad (42)$$

3. Results

3.1. Numerical Simulations

We analyzed the control of the "disabled operator-wheelchair" system, where the man is characterized by the model (11), ($k_h = 9.54$, $\tau = 0.1\ s$, $\beta = 1.5$) and the wheelchair has the electrical and mechanical parameters, as shown in Table A2.

Two cases will be examined. In the first case, the control system does not contain the controller Y_C, the disabled person directly controls the wheelchair orientation by changing the active wheel velocities. The movement on a linear trajectory with $\omega_1 = \omega_2 = 0.3\frac{rad}{s}$ is considered. For a sudden change in the direction of movement, the disabled man operates with a joystick, increases the velocity of the right wheel and decreases the velocity of the left wheel. The analysis of the trajectories, $\omega_1^{dis}(t)$, $\omega_2^{dis}(t)$, indicates the appearance of an over-steer phase and an oscillation regime. The Mittag-Leffler method [32] is used for MATLAB/SIMULINK simulation of the velocity trajectories (Figure 9). In the second case, a controller Y_C implements the control law (23). A controller with k_c =9.2, with $k_{c1} = 8$, $k_{c2} = 1.2$ is proposed. The inequality (25) is verified for $\sigma = 0.8$. A matrix $Q = qq^T$ with $q = col(2.5)$ is selected and the matrix P is obtained as a solution of Lyapunov equation $A^{*T}P + PA^*$ where the matrix A^* is a Hurwitz matrix, $Arg(eig(A^*)) > \frac{\pi}{2}$, (with $\lambda_1 = -33.48$, $\lambda_{2,3} = -6.2924 \mp i\ 6.0567$, $\lambda_{4,5} = -3.7086 \mp i\ 4.0386$, $\lambda_{6,7} = -7.3642 \mp i\ 5.7963$, $\lambda_{8,9} = -2.6358 \mp i\ 8.2765$, $\lambda_{10,11} = -1.3426 \mp i\ 2.4831$). The inequality (29) is verified for $\varrho = 28$, $\rho_{A_1P} = 0.17$. The frequential criteria (28) is verified for $\sigma = 0.8$. (Figure 9).

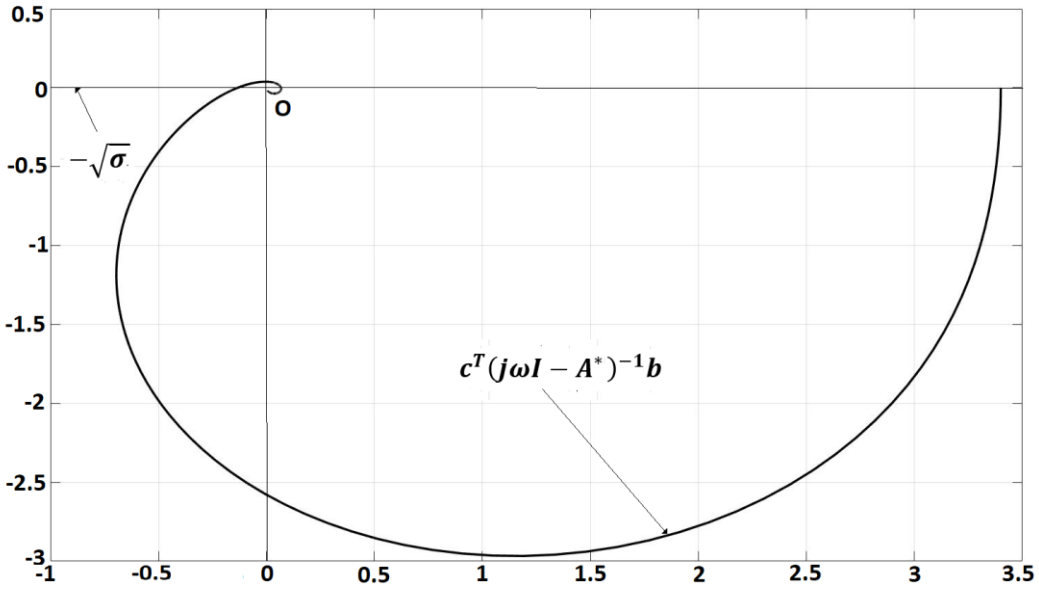

Figure 9. $\left(c^T(j\omega I - A^*)^{-1}b\right)$ plot.

The new $\omega_1^c(t)$, $\omega_2^c(t)$, trajectories are presented for comparison in the same figure (Figure 10). The increase of the movement quality can be easily noticed.

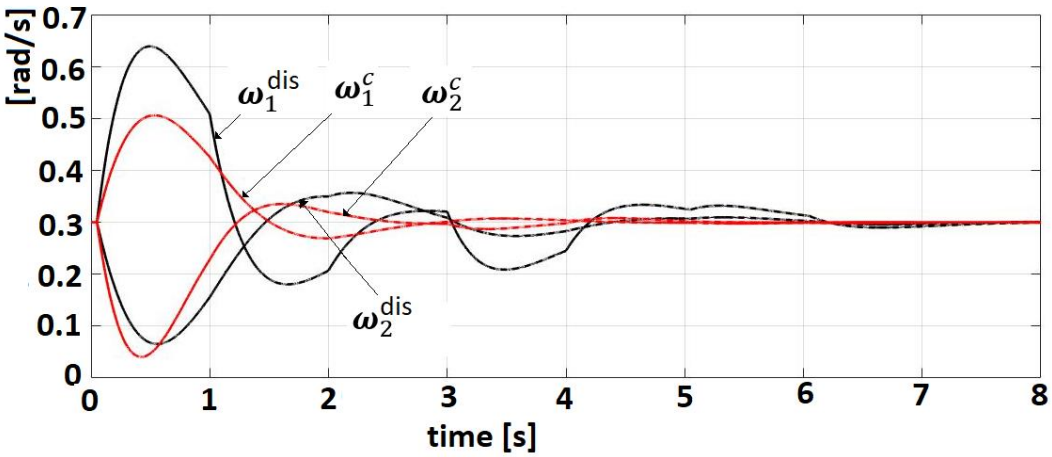

Figure 10. Velocity trajectories during the test motion (ω_1^{dis}, ω_2^{dis} : for disabled man without controller, ω_1^c, ω_1^c: for disabled man with controller).

3.2. Experimental Tests

The results of the previous sections were verified at the control of a wheelchair driven by a person with Parkinson's disability. This disability, like other similar ones caused by brain injuries, affects the control of movement. The driving function being characterized by rigid and uncontrollable movements of the hand, tremor and instability.

The experiments were performed on EZ Lite Cruiser Standard Model with rear wheel drive and joystick control of the direction of movement. These experiments tried to highlight the evolution of a wheelchair due to the inability of the disabled person to compensate for disturbances that occur during movement and improve the quality of motion by introducing an adequate control system. An experiment consists of data acquisition and their interpretation for an evolution on a test trajectory. A test trajectory has considered a movement that requires a sudden change of direction with 90° (step input), as seen in Figure 4. The tests performed were grouped into two categories. The first group of tests allowed for the identification of the disabled human model (with Parkinson's disease), according to the technique developed in Section 2.1. The second group of tests highlighted the performance obtained by introducing the controller analyzed in Section 2.3. The technical support of the experiments consisted of the Raspberry Pi4 System through which the acquisition and storage of angular velocities of the wheels in a motion trajectory and the implementation of the control law were performed. The stored data was subsequently processed (off-line) in a DELL 14 5000 computer using MATLAB toolboxes (Figure 3). The measured data of the angular velocities of the wheels are stored and then interpreted. Figure 5 presents the data of the trajectories for 10 experiments to identify the Parkinson disabled human model with $k_h = 9.54$, $\beta = 1.5$.

In the second part, a controller (42) with $k_c = 9.5$, $c_{h1} = 4.5$, $c_\omega^1 = 1.8$ and $c_\omega^2 = 0.8$ is implemented by Raspberry Pi4 System and a set of 10 tests are performed. The tracking error $e(t)$ is analyzed:

$$e(t) = \theta_{targ} - \theta(t) \tag{43}$$

where $\theta_{targ} = \frac{\pi}{2}$. The following quality index is proposed [36]

$$QI = \frac{1}{T}\sum_i |e_i|\Delta t_i \tag{44}$$

Figure 11 shows the errors $e(t)$ in three cases: with the Parkinson's disease human operator without controller, $e^P(t)$, in the case of the Parkinson's disease human operator

with controller, $e_c^P(t)$, and in the case of the healthy operator, $e^h(t)$. The experiment consists of 10 tests performed on two patients with Parkinson's disability. The results are summarized in Table A3 and are shown in Figure 12.

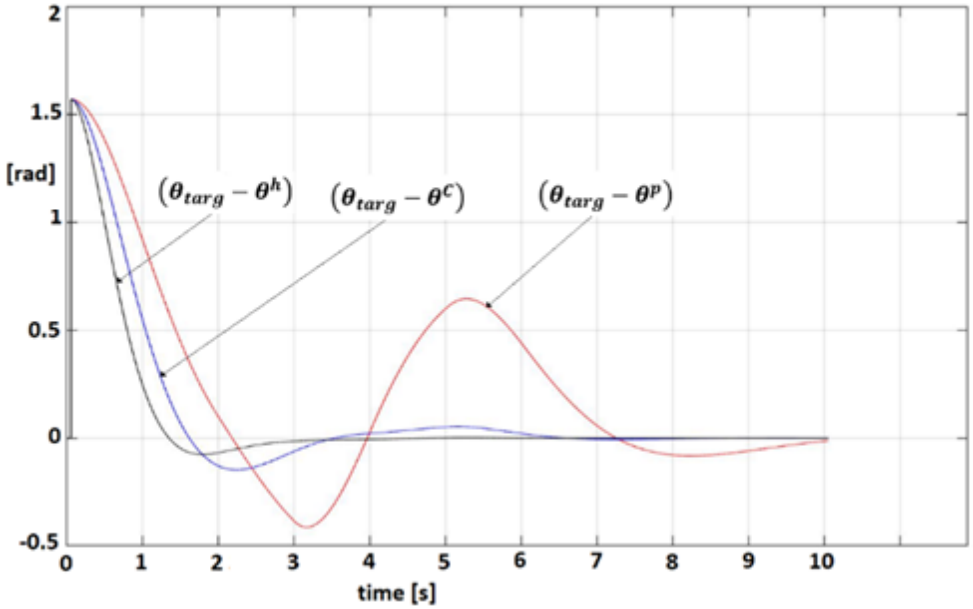

Figure 11. Error trajectories: $(\theta_{targ} - \theta^P)$ for the Parkinson's disease human operator without controller, $(\theta_{targ} - \theta^C)$ for the Parkinson's disease human operator with controller, $(\theta_{targ} - \theta^h)$ for the healthy operator.

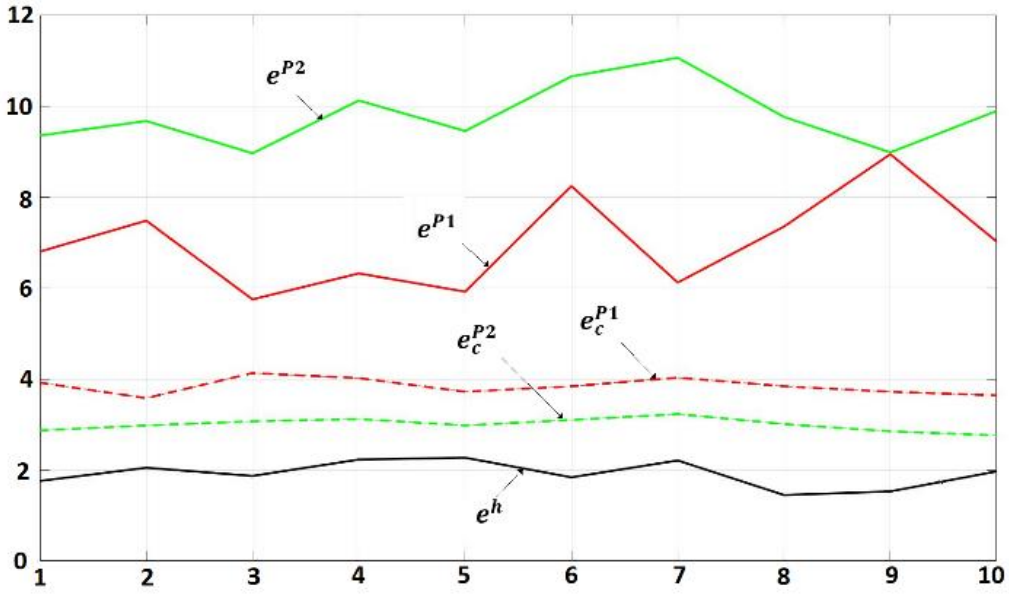

Figure 12. Experiment error.

4. Discussion and Conclusions

Mainstream literature includes numerous titles dedicated to human behavior in control systems. A selection of these papers is presented in Table 1.

A second order time delay FOM of the Human Operator behavior is developed in [4,6] and a fractional order control algorithm is analyzed. A $PI^{\lambda}D^{\mu}$ controller is proposed to ensure the desired performances of the control system. The time delay component is compensated and the quality control is investigated by Bode characteristics. The difficulty

of implementing the $PI^{\lambda}D^{\mu}$ controller is solved by the Oustaloup method. A Fractional Order Admittance Control is proposed in [7] for the physical human-robot interaction. The stability analysis of the closed-loop control system with human in-the loop is performed by using an extension of classical control theory. The delay time component is neglected. A flexible tuning strategy of the controller parameters is used. The dynamics of a coupled vehicle-driver system is analyzed in [20,23]. The model is a reduced-order non-linear model based on a separation between kinetic and kinematic driver control components. A linearized control law is used to implement "Linear Crossover Model". Classical PID controllers are implemented. A relation is established between the controller parameters and the relative dead time of the human. A suboptimal FOM description of human behavior in the coupled vehicle-driver system is studied in [2]. Human optimal control characteristics are analyzed considering psycho-physical limitations of a healthy driver. Prediction techniques are used to identify human model parameters. The optimal fractional-order PID controller based on specified gain and phase margins with a minimum integral squared error criterion is designed. A control algorithm is used to compensate for the time delay component. A state-space representation of the FOM for a human operator is discussed in [8]. Tuning and auto-tuning rules for fractional-order PID controllers are given. The tuning rules are obtained by establishing the relations between the human dynamics and the controller parameters. The design is focused on the maximization of the integral gain with a constraint on maximum sensitivity. A rational approximation of the time delay component is used.

This paper uses frequency techniques to identify the dynamic model of the "Parkinson's disease person-wheelchair" system. The fractional order equations of the "Parkinson's man-wheelchair" are inferred. The crossover model with a fractional order exponent $\beta = 1.5$ is evaluated by Bode diagram analysis of the wheelchair evolutions driven by a person with Parkinson's disease on a test trajectory. A control system is proposed to eliminate the inability of the human operator to ensure the movement of higher quality performances. The stability of the control system is demonstrated by the Lyapunov techniques. Frequency criteria derived from the Yakubovici-Kalman-Popov Lemma are used to verify the performance of the control system. Two control solutions are proposed: a FOM controller (42) and a PD-IOM controller (43) implemented by measurable variables. Both control solutions display similar performances by tuning the control parameters [28], but the IOM control is preferred due to the implementation facilities of the controller. An experimental technique for analyzing the movement performance is developed and a quality index is proposed to evaluate these experiments. The values of this index on the tests performed on Parkinson's patients confirm the correctness of the proposed solutions.

New investigation methods for other categories of people with functional disabilities will be developed in the future. Also, the possibility of including humans in the general structure of the controller will be studied with the man-machine architecture being analyzed as a hierarchical system.

Author Contributions: Conceptualization, M.I. and I.D.; methodology, N.P.; software, D.P.; validation, M.I. and N.P.; formal analysis, I.D.; investigation, D.P.; resources, M.I.; data curation, D.P.; writing—original draft preparation, N.P.; writing—review and editing, D.P.; visualization, M.I.; supervision, I.D.; project administration, N.P.; funding acquisition, M.I. All authors have read and agreed to the published version of the manuscript.

Funding: This research was funded by ROMANIAN SOCIETY OF ROBOTICS, grant number 325/2021.

Data Availability Statement: Not applicable.

Conflicts of Interest: The authors declare no conflict of interest.

Appendix A

Table A1. Human gain coefficient k_h.

Human gain coefficient k_h (Patient 1)					
Experiment	1	2	3	4	5
k_h	15.84	12.04	6.80	7.01	13.01
Experiment	6	7	8	9	10
k_h	6.29	7.82	8.01	9.24	8.73
Human gain coefficient k_h (Patient 2)					
Experiment	1	2	3	4	5
k_h	11.36	9.12	7.23	8.42	8.88
Experiment	6	7	8	9	10
k_h	7.95	8.53	12.12	6.56	11.32
Phase angle φ (Patient 1)					
Experiment	1	2	3	4	5
φ [*rad*]	3.843	4.012	3.910	4.002	3.768
Experiment	6	7	8	9	10
k_h	3.891	4.123	4.014	3.901	3.927
Phase angle φ (Patient 2)					
Experiment	1	2	3	4	5
φ [*rad*]	4.134	3.761	3.812	3.954	4.233
Experiment	6	7	8	9	10
k_h	3.762	3.842	3.954	3.910	4.213

Table A2. Wheelchair Electrical and Mechanical Parameters.

Parameter.		**Value**
J	Drive System Inertia	0.270 kg·m^2
R_a	Armature resistance	0.2957 Ω
L_a	Armature inductance	0.082 mH
v	Viscous friction coefficient	0.1044 Nm s/rad
k_e	Speed constant	1.685 rad/s/V
k_t	Torque constant	1.4882 Nm/A
m	Wheelchair mass	98 kg

Appendix B

Table A3. QI for experimental tests.

Experiment	**Test 1**	**Test 2**	**Test 3**	**Test 4**	**Test 5**
Parkinson's Patient 1 (without controller)	6.80	7.48	5.75	6.32	5.92
Experiment	**Test 6**	**Test 7**	**Test 8**	**Test 9**	**Test 10**
Parkinson's Patient 1 (without controller)	8.24	6.12	7.35	8.94	7.02

Table A3. *Cont.*

Experiment	Test 1	Test 2	Test 3	Test 4	Test 5
Parkinson's Patient 1 (with controller)	3.92	3,58	4.13	4.02	3.72
Experiment	**Test 6**	**Test 7**	**Test 8**	**Test 9**	**Test 10**
Parkinson's Patient 1 (with controller)	3.84	4.03	3.82	3.72	3.64

Appendix C

Mathematical Preliminaries

Consider the fractional order system

$$D^{\beta}z(t) = Az(t)$$

where $D^{\beta}z(t)$ is the Caputo derivative of $z(t)$ for $0 < \beta < 1$.

Definition 1. *The matrix A is Hurwitz stable if*

$$Arg(eig(A)) > \frac{\pi}{2} \tag{A1}$$

Definition 2. *The matrix A is β-fractional order stable if*

$$Arg(eig(A)) > \beta\frac{\pi}{2}$$

Theorem 2 ([28,30]). *The system* (1)*, where A is β-fractional order stable, is asymptotically stable.*

Theorem 3 ([28,33]). *The system $D^{\beta}z(t) = f(z(t))$, $z(t_0) = z_0$ is asymptotically stable if there exists a continuously differentiable function $V(t,z)$ that satisfies*

$$\alpha_1\|z\|^2 \leq V(t,z(t)) \leq \alpha_2\|z\|^2$$

$$D^{\beta}V(t,z(t)) \leq -\alpha_3\|z\|^2$$

where α_1, α_2, α_3 are positive constants, $0 < \beta < 1$.

Lemma 1. ([32,33]). *Let $z(.) \in R^n$ be a differentiable vector function. Then, the following inequality holds:*

$$\frac{1}{2}D^{\beta}\left[z^T(t)z(t)\right] \leq z^T(t)D^{\beta}z(t),\ \beta \in (0,1),\ t \geq t_0$$

Lemma 2. *Yakubovici-Kalman-Popov (YKP) Lemma [35]. Given a positive number $\sqrt{\sigma}$, the vectors b, c, a Hurwitz matrix A, then a symmetric matrix P and a vector q satisfying.*

$$\left(A^TP + PA\right) = -qq^T$$

$$Pb - \frac{1}{2}c = \sqrt{\sigma}q$$

exist if and only if

$$Re\left(c^T(j\omega\mathrm{I} - A)^{-1}b\right) \geq -\sqrt{\sigma},\ \forall\omega \in (-\infty, +\infty)$$

References

1. McRuer, D.T.; Jex, H.R. A Review of Quasi-Linear Pilot Models. *IEEE Trans. Hum. Factors Electron.* **1967**, *3*, 235–249. [CrossRef]
2. Kleinman, D.I.; Baron, S.; Levison, W.H. An Optimal Control of Human Response. *Automatica* **1970**, *6*, 357–369. [CrossRef]
3. Mabrok, M.A.; Mohamed, H.K.; Abdel-Aty, A.-H.; Alzahrani, A.S. Human models in human-in-the-loop control systems. *J. Intell. Fuzzy Syst.* **2020**, *38*, 2611–2622. [CrossRef]
4. Huang, J.; Chen, Y.; Li, H.; Shi, X. Fractional Order Modeling of Human Operator Behavior with Second Order Controlled Plant and Experiment Research. *IEEE/CAA J. Autom. Sin.* **2016**, *30*, 271–280.
5. Martínez-García, M.; Gordon, T. Human control of systems with fractional order dynamics. In Proceedings of the 2016 IEEE International Conference on Systems, Man, and Cybernetics (SMC), Budapest, Hungary, 9–12 October 2016.
6. Garcia, M.M.; Gordon, T.; Shu, L. Extended Crossover Model for Human-Control of Fractional Order Plants. *Fault Diagn. Control Cyber-Phys. Syst.* **2017**, *5*, 27623–27634.
7. Aydin, Y.; Tokatli, O.; Patoglu, V.; Basdogan, C. Stable Physical Human-Robot Interaction Using Fractional Order Admittance Control. *IEEE Trans. Haptics* **2017**, *7*, 2. [CrossRef] [PubMed]
8. Kang, H.G.; Seong, P.H. Information theoretic approach to man-machine interface complexity evaluation. *IEEE Trans. Syst. Man Cybern. Part A Syst. Hum.* **2001**, *31*, 163–171. [CrossRef]
9. Plöchl, M.; Edelmann, J. Driver models in automobile dynamics application. *Veh. Syst. Dyn.* **2007**, *45*, 699–741. [CrossRef]
10. Kondo, M.; Ajimine, A. Driver's sight point and dynamics of the 900 driver-vehicle-system related to it. *SAE Tech. Pap.* **1968**, 680104, Corpus ID: 61990044. [CrossRef]
11. Becedas, J. Brain–Machine Interfaces: Basis and Advances. *IEEE Trans. Syst. Man Cybern. Part C Appl. Rev.* **2012**, *42*, 825–836. [CrossRef]
12. Prokop, G. Modeling Human Vehicle Driving by Model Predictive Online Optimization. *Veh. Syst. Dyn.* **2001**, *35*, 19–53. [CrossRef]
13. Salvucci, D.D.; Gray, R. A two-point visual control model of steer-906 ing. *Perception* **2004**, *33*, 1233–1248. [CrossRef] [PubMed]
14. Parasuraman, R.; Sheridan, T.; Wickens, C. A model for types and levels of human interaction with automation. *IEEE Trans. Syst. Man Cybern. Part A Syst. Hum.* **2000**, *30*, 286–297. [CrossRef] [PubMed]
15. Hollingworth, A.; Williams, C.; Henderson, J. To see and remember: Visually specific information is retained in memory from previously attended objects in natural scenes. *Psychon. Bull. Rev.* **2001**, *8*, 761–768. [CrossRef] [PubMed]
16. Schlick, C.; Winkelholz, C.; Motz, F.; Luczak, H. Self-generated complexity and human-machine interaction. *IEEE Trans. Syst. Man Cybern. Part A Syst. Hum.* **2005**, *36*, 220–232. [CrossRef]
17. Mabrok, M.; Mohamed, H.; Abdel, A.H.; Alzahrani, A. Human models in human-in-the-loop control systems. *J. Intell. Fuzzy Syst.* **2019**, *38*, 2611–2612. [CrossRef]
18. Liu, Y.K.; Zhang, Y.M. Control of human arm movement in machine-human cooperative welding process. *Control Eng. Pract.* **2014**, *32*, 161–171. [CrossRef]
19. Tejado, I.; Valério, D.; Pires, P.; Martins, J. Fractional order human arm dynamics with variability analyses. *Mechatronics* **2013**, *23*, 805–812. [CrossRef]
20. Gordon, T.J. Nonlinear crossover model of vehicle directional control. In Proceedings of the 2009 American Control Conference, St. Louis, MO, USA, 10–12 June 2009; pp. 451–456.
21. Hollingworth, A.; Richard, A.M.; Luck, S.J. Understanding the function of visual short-term memory: Transsaccadic memory, object correspondence, and gaze correction. *J. Exp. Psychol. Gen.* **2008**, *137*, 163. [CrossRef]
22. Pew, R.W. *Some History of Human Performance Modeling*; Oxford University Press: Oxford, UK, 2007; pp. 29–44. [CrossRef]
23. Li, W.; Sadigh, D.; Shankar Sastry, S.; Sanjit, S.A. Synthesis for Human-in-the-Loop Control Systems. In *International Conference on Tools and Algorithms for the Construction and Analysis of Systems*; Springer: New York, NY, USA, 2014; TACAS 2014; pp. 470–484, Lecture Notes in Computer Science, Book Series LNTCS; Volume 8413.
24. Aidin, Y.; Tokatli, O.; Patoglu, V.; Basdogan, C. Fractional Order Admittance Control for Physical Human-Robot Interaction. In Proceedings of the 2017 IEEE World Haptics Conference (WHC), Munich, Germany, 6–8 June 2017.
25. Laurense, V.; Pool, D.; Damveld, H.; Van Paassen, M.; Mulder, M. Effects of Controlled Element Dynamics on Feedforward Manual Control. *IEEE Trans.* **2015**, *45*, 253–265.
26. Wolm, P. Dynamic Stability Control of Front Wheel Drive Wheelchair Using Solid State Accelerometer and Gyroscope. Ph.D. Thesis, University of Canterbury, Canterbury, New Zealand, 2009.
27. Ivanescu, M.; Popescu, N.; Channa, A.; Poboroniuc, M. Exoskeleton Hand Control by Fractional Order Models. *Sensors* **2019**, *19*, 4608. [CrossRef] [PubMed]
28. Petras, I. *Fractional-Order Nonlinear Systems, Modeling, Analysis and Simulation*; Higher Education Press: Beijing, China; Springer: Berlin/Heidelberg, Germany, 2011.
29. Naujoks, F.; Wiedemanna, K.; Schomiga, N.; Jaroschb, O.; Gold, C. Expert-based controllability assessment of control transitions from automated to manual driving. *MethodsX* **2018**, *5*, 579–592. [CrossRef] [PubMed]
30. Aguila-Camacho, N.; Duarte-Mermoud, M.; Callegos, J. Lyapunov functions for fractional order systems. *Commun. Nonlinear Sci. Numer. Simul.* **2014**, *19*, 2951–2957. [CrossRef]
31. Li, Y.; Chen, Y.; Podlubny, I. Stability of fractional-order nonlinear dynamic systems: Lyapunov direct method and generalized Mittag–Leffler stability. *Comput. Math. Appl.* **2010**, *59*, 1810–1821. [CrossRef]

32. Argarwal, R.; Hristova, S.; O'Regan, D. Lyapunov functions and strict stability of Caputo fractional differential equations. *Adv. Differ. Equ.* **2015**, *346*, 2–20.
33. Agarwal, R.; Hristova, S.; O'Reagan, D. Remarks on Lyapunov functions to Caputo fractional neural networks. *Ann. Acad. Rom. Sci.* **2018**, *10*, 169–176.
34. Monje, C.; Chen, Y.Q.; Vinagre, B.; Xue, D.; Feliu, V. *Fractional-Order Systems and Controls, Fundamental and Applications*; Springer: London, UK, 2010.
35. Khalil, H. *Nonlinear Systems*; Prentice Hall: Hoboken, NJ, USA, 2002.
36. Lyman Ott, R.; Longnecker, M.T. *An Introduction to Statistical Methods and Data Analysis*; Cengage Learning, Inc.: Boston, MA, USA, 2006; ISBN 978-1305269477.